Flexible Array Coil for Cervical and Extraspinal (FACE) for MR Neurography of the Occipital Nerves at 3 Tesla

Yenpo Lin, Ek T. Tan, Martijn Lunenburg, Shayna Turbin, Lisa Gfrerer and Darryl B. Sneag

AJNR Am J Neuroradiol published online 21 November 2024
http://www.ajnr.org/content/early/2024/11/21/ajnr.A8597

Flexible Array Coil for Cervical and Extraspinal (FACE) for MR Neurography of the Occipital Nerves at 3 Tesla

Yenpo Lin, Ek T. Tan, Martijn Lunenburg, Shayna Turbin, Lisa Gfrerer, Darryl B. Sneag

ABSTRACT

This technical report describes use of a novel, conformable receive-only radiofrequency coil for 3T magnetic resonance (MR) neurography in a cohort of patients with occipital neuralgia. Applying a sub-millimeter, isotropic three-dimensional double-echo steady-state sequence, detailed visualization of the occipital nerves and associated pathologies could be achieved.

ABBREVIATIONS: ABC = definition; XYZ = definition. FACE = Flexible Array coil for Cervical and Extraspinal; DESS = double-echo steady-state; C1, C2, C3 = First, second, and third cervical vertebrae respectively.

Received month day, year; accepted after revision month day, year.
From the Department of Radiology and Imaging, Hospital for Special Surgery, New York, NY, USA (Y.L., E.T.T., S.T., D.B.S.), Department of Medical Imaging and Intervention, Chang Gung Memorial Hospital, Taoyuan, Taiwan (Y.L.), Tesla Dynamic Coils, Zaltbommel, The Netherlands (M.L.) and Division of Plastic and Reconstructive Surgery, Weill Cornell Medicine, New York, USA (L.G.)

This work was partially funded by the HSS Innovations Department. A portion of this work is related to US Provisional Patent 63/058,725, filed on July 30, 2020 (E.T.T., D.B.S.). E.T.T. and D.B.S. also receive institutional research support from GE HealthCare and Siemens. M.L. is an employee of Tesla Dynamic Coils. L.G. served as a consultant for BioCircuit Technologies.

Please address correspondence to Darryl B. Sneag, MD, Department of Radiology and Imaging, Hospital for Special Surgery, 535 E70th St. New York, NY, 11101, USA; sneagd@hss.edu.

INTRODUCTION

Occipital neuralgia may result from pathologic changes of the greater occipital nerve (GON), lesser occipital nerve (LON), and/or third occipital nerve (TON). Targeted interventions, such as analgesic injections or surgical decompression, can provide significant pain relief.[1] However, as clinical symptoms of occipital neuralgia overlap with those of other headache disorders,[2] arriving at a definitive diagnosis can be challenging.

Magnetic resonance (MR) neurography has emerged as a promising technique for evaluating patients with occipital neuralgia, which may exhibit asymmetric hyperintensity and caliber changes of the GON as it emerges from the semispinalis capitis muscle and trapezius fascia to then enter the overlying subcutaneous fat.[3] Additionally, MR neurography can identify neuroma formation following iatrogenic injury.[4–6] Three-dimensional (3D) sequences such as T2-weighted turbo/fast spin echo (TSE/FSE) and reversed fast imaging in steady-state free precession (PSIF) are often employed in MR neurography to delineate the circuitous courses of the small peripheral nerves in the head and neck.[3,7] An alternative 3D double-echo steady state (DESS) sequence, similar to PSIF, is more time-efficient as it acquires two echoes with minimal increase in repetition time, and in theory, can provide the high spatial resolution needed for visualizing the occipital nerves, from the C2-3 dorsal root ganglia (DRG) to their subcutaneous innervations.[8] Further image quality enhancement for 3D DESS sequences have also been demonstrated using deep learning and image combination reconstructions.[9] Even when applying these advanced reconstruction techniques, our experience with the DESS sequence using a conventional, 21-channel rigid head-neck-unit (HNU) is that insufficient signal-to-noise ratio (SNR) is available to acquire submillimeter, isotropic resolution.

The development of flexible coil technologies can improve conformability of surface coils to increase SNR, and enables specialized coil designs that can be optimized to specific anatomical regions.[10] Recently, a 23-channel Flexible Array for Cervical and Extraspinal (FACE) MRI was developed for the posterior and lateral neck regions.[11] The FACE coil demonstrated superior SNR and improved parallel imaging performance compared to a conventional 21-channel HNU.[11] Its use in patients with occipital neuralgia is expected to improve confidence in imaging the occipital nerves and identifying related pathologies. This work describes the application of the FACE coil, and acquisition and reconstruction algorithms, for MR neurography evaluation of a cohort of patients with occipital neuralgia.

MATERIAL AND METHODS

This prospective study was approved by our Institutional Review Board with written informed consent obtained for utilizing the prototype coil. The study adhered to the Strengthening the Reporting of Observational Studies in Epidemiology (STROBE) reporting guidelines. Between November 2022 and February 2024, patients with clinically suspected occipital neuralgia who underwent MR neurography on a 3T MRI system (Signa Premier, GE HealthCare, Waukesha, WI, USA) were enrolled.

Copyright 2024 by American Society of Neuroradiology.

The FACE coil[11](Tesla Dynamic Coils, Zaltbommel, Netherlands) comprises a flexible mask for optimal neck contouring and a rigid posterior headrest housing, designed to integrate with the patient table inlay in a manner similar to the HNU (Fig. 1). By utilizing a biconical, conformal 2D array-shape, the coil layout achieves circumferential coverage of the neck, extending from the skull base to the T1-2 thoracic segments, with a particular focus on the lateral and posterior cervical regions. This allows the coil to conform closely to the complex contours of this anatomical area. Preliminary work has shown that the FACE provides superior SNR as compared to a rigid 21-channel HNU (Fig. 1).

MR Neurography Protocol

A coronal 3D DESS sequence with the 2 echoes separately reconstructed was performed within 4.5 minutes (time to echo (TE) = 5/9 msec; repetition time (TR) = 15 msec; acquired matrix = 256×256 to 316×316; field-of-view (FOV) = 20.0×20.0 cm; slice thickness = 0.6-0.8 mm; receiver bandwidth (RBW) = 139.50-162.7 Hz/pixel, parallel imaging factors = 2×2). High, isotropic spatial resolutions (0.6-0.8 mm) were acquired with DESS, adapted to the patient's body habitus. The 3D DESS sequence was initially obtained at 0.8 mm^3 resolution. During real-time monitoring, for some cases the sequence was repeated at 0.6 or 0.7 mm^3 resolution to further delineate the anatomy and any associated pathology at the radiologist's discretion (Fig. 2). DESS acquisitions were also reconstructed using a 3D prototype of a deep learning reconstruction algorithm (AIR™ Recon DL, GE HealthCare) to enhance SNR and edge sharpness.[9] A geometric combination of the 2 echoes was used to further enhance SNR while retaining T2-weighting.[9]

The MR neurography protocol used in this study also included axial and coronal 2D intermediate-weighted FSE (parameters: TE = 25-30 msec; TR = 3000-5000 msec; ETL = 16; acquired matrix = 512×352; FOV = 16-20×16-20 cm; slice thickness = 2-2.5 mm; RBW = 244 Hz/pixel) and axial T2-weighted Dixon FSE (parameters: TE = 85 ms; TR = 3000-4500 ms; ETL = 15; acquired matrix = 320×224; FOV = 16×16 cm; slice thickness = 2 mm; RBW = 244.1 Hz/pixel). Furthermore, a 1 mm, isotropic zero-echo time (ZTE) (parameters: TE = 0 ms; TR = 500 ms; acquired matrix = 224×224; FOV = 24×24 cm; slice thickness = 1 mm; RBW = 488.28 Hz/pixel) sequence was acquired to provide visualization of bony landmarks relative to nerves for aiding in surgical planning or other interventions (Fig. 3).

MR Neurography Interpretation

All images were reviewed postoperatively and jointly by 2 musculoskeletal radiologists (Y.L. and D.B.S.) with 2 and 9 years' MR neurography experience, respectively. Both radiologists were blinded to the patient's history and subsequent surgical findings. Visualization of the GON was evaluated (yes/no) at the following 3 sites similar to previous studies[8,12]: the posterior edge of the obliquus capitis inferior muscle, the entry point to the semispinalis capitis muscle, and immediately deep to the trapezius muscle fascia. Visualization of the LON was also recorded (yes/no) at 3 sites: its emergence from the surface of the levator scapulae muscle, the posterior edge of the sternocleidomastoid muscle, and the level of the occipital protuberance. Visualization of the TON was recorded (yes/no) at 2 sites, from deep and superficial to the semispinalis muscle.

CASE SERIES RESULTS

Thirteen consecutive patients (8 women) with a median age of 52 years (range 35-73) and clinically suspected occipital neuralgia underwent neck MR neurography. Demographic and clinical characteristics of the patients, along with their MR neurography findings and surgical outcomes, are summarized in Online Supplemental Data. The median time from symptom onset to imaging was 70 months (range: 7-399 months). Of the 13 patients, 7 had a history of prior surgery, including 3 with prior cervical spine surgery and 4 with prior occipital nerve decompression.

On MR neurography, all segments of GONs were visualized to their superficial course above the trapezius muscle fascia, except in 3 patients with neuroma findings, which are described subsequently. However, segments of LONs beyond the posterior edge of the sternocleidomastoid muscle were not visualized in 5 patients (2 unilateral, 3 bilateral). Additionally, TON segments superficial to the semispinalis capitis muscle were not visualized bilaterally in 3 patients. Notably, in one of these patients, bilateral LON and TON were obscured by instrumentation from prior cervical spine surgery.

In patients with prior surgery, MR neurography identified occipital terminal neuromas, defined as the nerve terminating in a focally enlarged mass, in 3 patients (1 following cervical spine surgery and 2 following occipital nerve decompression). These neuromas were located deep to the semispinalis capitis muscle and in proximity to prior surgical incisions. Unilateral GON neuromas were found in 2 patients, while neuromas of both the GON and TON were seen in 1 patient (Fig. 4). All neuromas were surgically confirmed and resected, except for 1 unilateral GON neuroma, which the surgeon deemed not directly related to the patient's symptoms. In another case with prior cervical spine surgery, while the GON demonstrated normal signal intensity, arthrosis with osteophyte formation at the right C1-2 lateral mass articulation resulting in severe compression of the C2 DRG was deemed the most likely etiology of the patient's neuralgia.

Among the 6 patients without antecedent surgery, MR neurography in 1 patient revealed an enlarged and hyperintense right LON (Fig. 5), consistent with the patient's right occipital neuralgia. The asymptomatic, contralateral LON appeared normal.

DISCUSSION

This study describes the use of a prototype, highly flexible array coil, combined with a high-resolution protocol, for 3D MR neurography of the occipital nerves. Together, these techniques were used to evaluate potential surgical candidates in patients experiencing chronic occipital neuralgia.

A previous study of occipital MR neurography demonstrated the efficacy of a 0.9 mm-isotropic 3D reversed fast imaging with steady-state precession (PSIF), a gradient echo sequence with contrast analogous to the second echo of DESS, to detect increased signal intensity and size alterations of the GON in patients with unilateral, occipital neuralgia.[13] Another study utilizing DESS (approximately 0.5 × 0.8 × 0.9 mm spatial resolution) demonstrated its effectiveness in defining the GON posterior to the trapezius fascia and the LON at the level of the occipital protuberance, albeit in patients with suspected salivary gland lesions, not occipital neuralgia.[8] Given the small size of the native occipital nerves (~5 mm in diameter)[1,14], we instead targeted an approach utilizing a 3D DESS sequence, with isotropic resolution as high as 0.6 mm, to increase the confidence of localizing neuromas in subjects with prior decompression surgery. Additionally, we evaluated the visualization of the TON, including a case of TON neuroma within our cohort, which to our knowledge is rarely reported on MR neurography. Previous findings using the FACE coil demonstrated suitability of the coil for cervical spine imaging as well.[11] This functionality is particularly beneficial in patients with occipital neuralgia, as arthrosis at the C1-2 lateral mass articulation is known to result in compression of the C2 DRG[15], and was the likely cause for symptoms in one of the patients of this case series.

This study was limited by its small sample size. Further studies with larger cohorts and robust study designs are necessary to confirm the efficacy of the FACE coil in diagnosing occipital neuralgia. Furthermore, this study did not include comparisons of image quality delineating the effects of improved SNR owing to the deep learning and geometric image combination reconstructions applied to the DESS sequence. However, the comparisons of the effects from both deep learning and geometric image combination effects had previously been comprehensively demonstrated in the brachial plexus and lumbosacral plexus.[9,16] Another limitation was that no systematic, quantitative comparisons were made between the signal intensity and size of abnormal and normal occipital nerve segments, primarily due to the limited number of positive findings in our cohort. Therefore, the efficacy for using the FACE coil on diagnostic interpretability in these nerves (i.e. signal and morphology) remains to be determined, as there are few studies to non-invasively establish normative values for signal intensity and size in MR neurography.[7]

CONCLUSION

The 23-channel FACE coil, in combination with advanced imaging reconstruction methods, allowed excellent visualization of the GON and neuromas in all occipital neuralgia patients, with or without a history of preceding cervical surgery, and the LON and TON in the majority of patients at high spatial resolution (0.6-0.8 mm isotropic). Additional research with larger cohorts is required to validate these results and further assess its clinical utility.

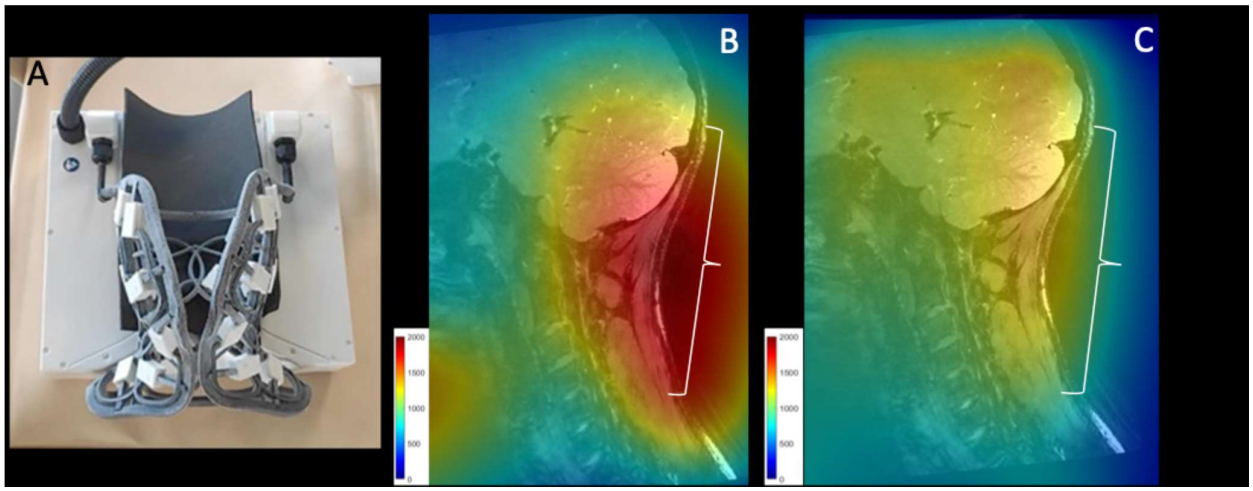

FIG 1. Comparison of signal-to-noise ratio (SNR) maps overlaid on sagittal double echo steady state (DESS) images of the neck in the same subject. The FACE coil (A) with flexible mask and a rigid posterior head-rest housing, which demonstrates superior SNR in the posterolateral neck regions (B) compared to the conventional HNU coil (C). The brackets in panels (B) and (C) indicate the imaging target regions of occipital nerves

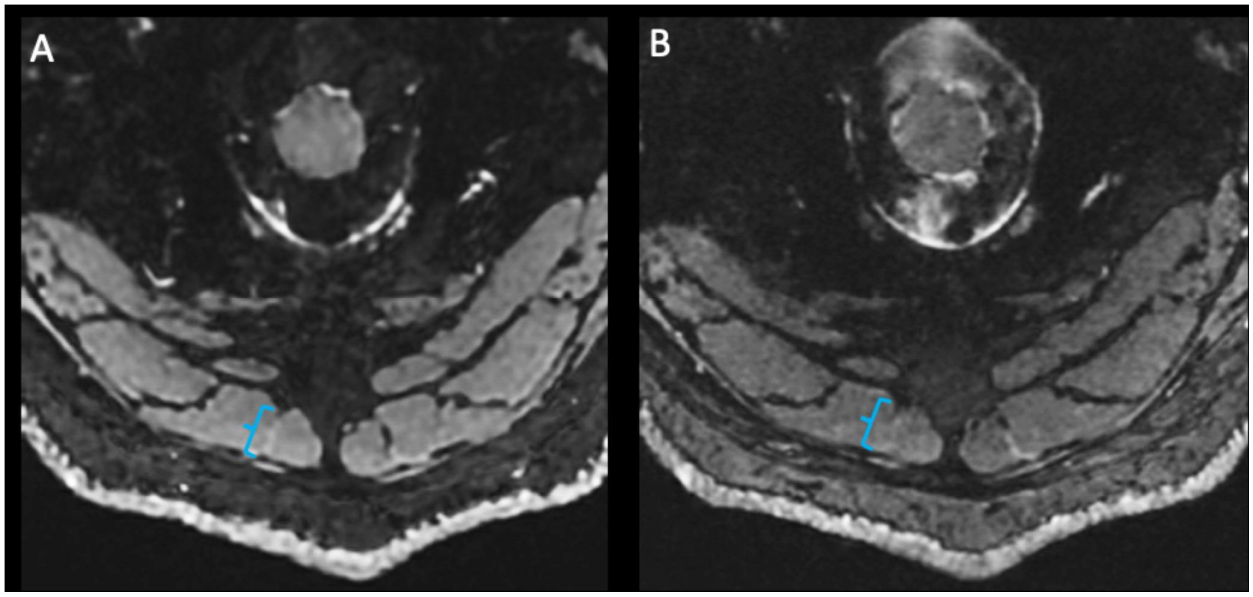

FIG 2. Comparison of different spatial resolutions in a 36-year-old man with chronic occipital neuralgia. Axial DESS images with 0.8×0.8×0.8 mm (A) and 0.6×0.6×0.6 mm (B) resolution show that while anatomical detail is sharper in (B), the right occipital nerve traversing the semispinalis capitis muscle (highlighted by brackets) appears subtly more conspicuous in (A).

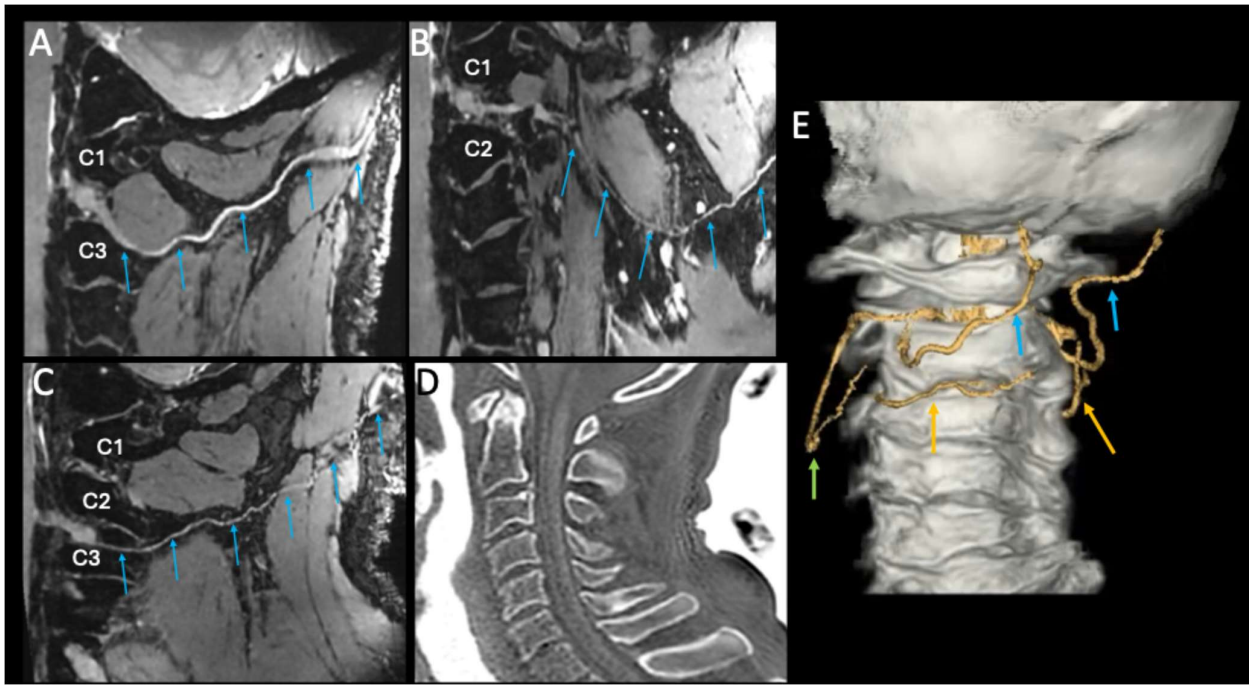

FIG 3. Fused rendering of 3D MR neurography and zero-to-echo (ZTE) images in a 45-year-old man, performed for protocol optimization. (A-C) Curved multiplanar reconstruction images from a 0.6 mm isotropic double echo steady state (DESS) sequence of the (A) greater occipital nerve (GON, arrows), (B) lesser occipital nerve (LON, arrows) and (C) third occipital nerve (TON, arrows). (D) Sagittal 1 mm isotropic ZTE image displays the relevant vertebral body levels. (E) Fused-rendering of the DESS and ZTE images demonstrates the spatial relationships of the bilateral GONs (blue arrows), left LON (green arrow) and TONs (orange arrows) at the corresponding vertebral levels.

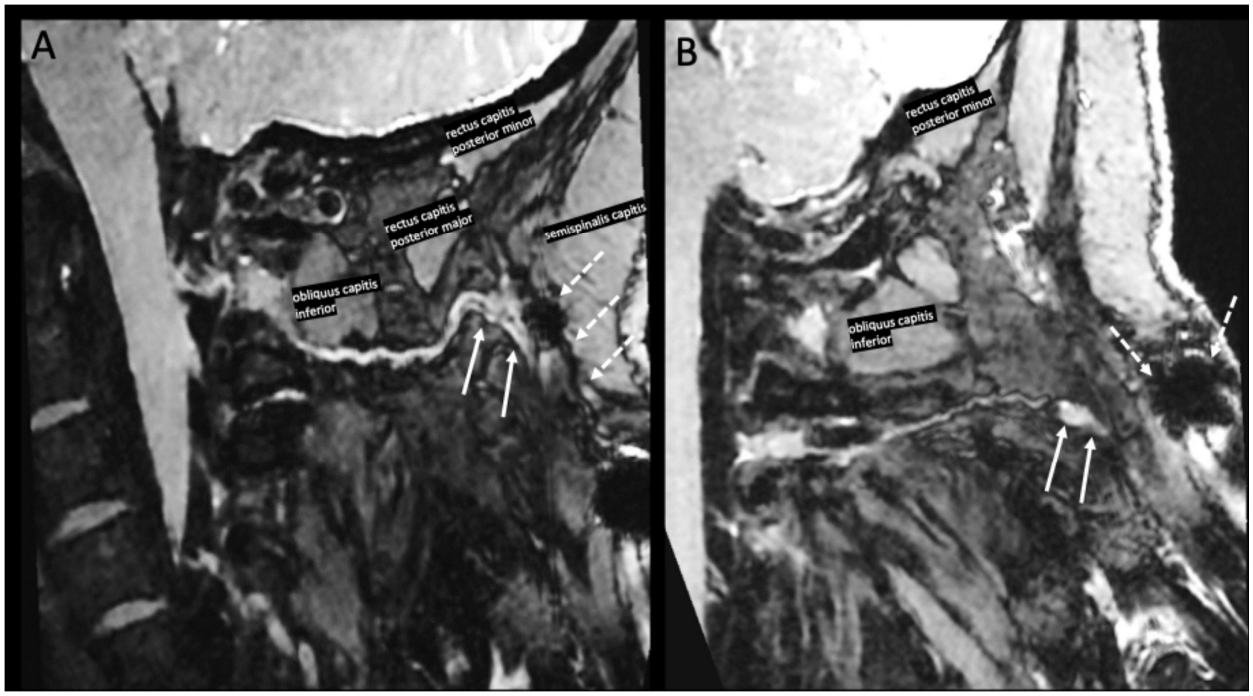

FIG 4. 39-year-old female with a history of left greater occipital nerve (GON) decompression. Curved multiplanar reconstruction (cMPR) images (A,B) from a 0.6 mm isotropic double echo steady state sequence demonstrates terminal neuromas of both the left GON (solid arrows, A) and left third occipital nerve (TON) (solid arrows, B). The GON neuroma is located deep to the semispinalis capitis muscle and prior surgical incisions (dashed arrows, A), while the TON neuroma is situated adjacent to a focus of susceptibility artifact (dashed arrows, B). Surrounding muscles are labeled for anatomical reference.

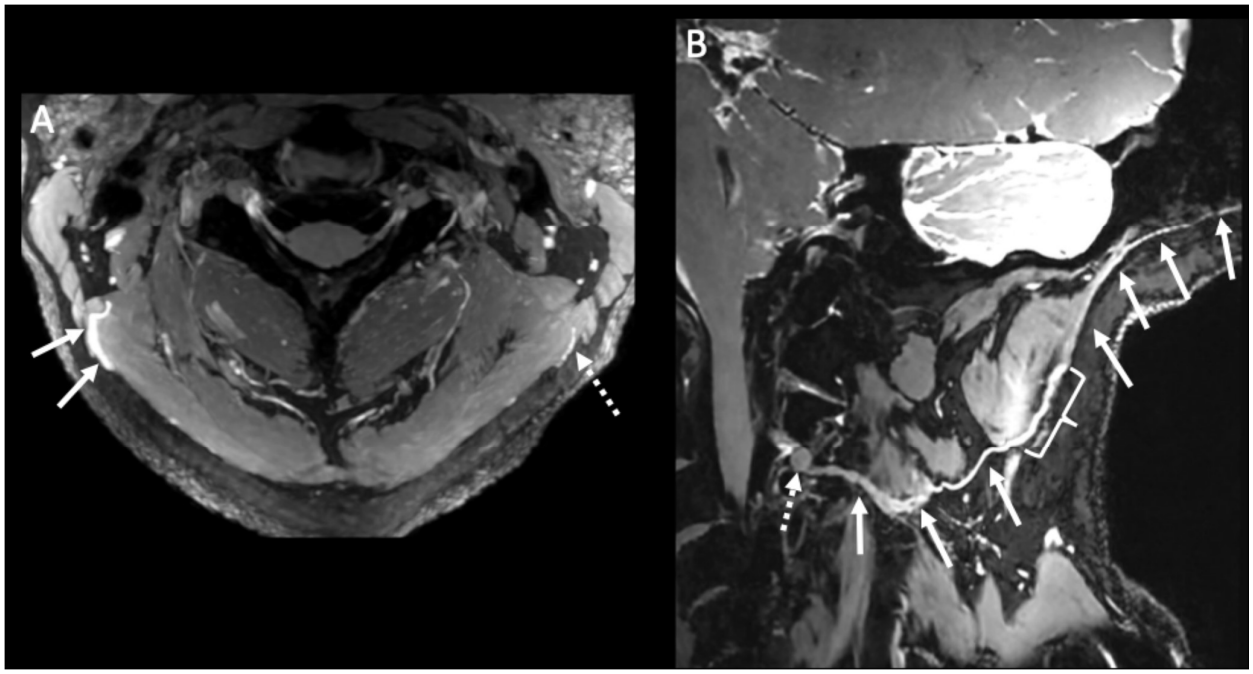

FIG 5. 68-year-old woman with a 2-year history of right occipital neuralgia. (A) Axial T2-weighted two-dimensional (2D) maximal intensity projection (MIP) Dixon image demonstrates short segment signal hyperintensity (solid arrows) of the right lesser occipital nerve (LON) as it traverses between the sternocleidomastoid and splenius capitis muscles. Note the normal size and signal intensity of the left LON (dashed arrow). (B) Curved multiplanar reconstruction image from a 0.7 mm isotropic double echo steady state acquisition reveals the course of the right LON from the subcutaneous fat overlying the scalp to the C2 dorsal root ganglion (dashed arrow) and confirms the segmental enlargement and hyperintensity (bracket) seen on the 2D Dixon image (A).

ACKNOWLEDGMENTS

The authors thank the HSS Innovation Institute for funding this work. The authors also thank Fraser Robb, PhD and Jana Vincent, PhD, for performing safety testing of the coil, and Yan Wen, PhD for his technical support.

REFERENCES

1. Ducic I, Hartmann EC, Larson EE. Indications and Outcomes for Surgical Treatment of Patients with Chronic Migraine Headaches Caused by Occipital Neuralgia. Plast Reconstr Surg 2009;123:1453–61.
2. Headache Classification Committee of the International Headache Society (IHS) The International Classification of Headache Disorders, 3rd edition. Cephalalgia 2018;38:1–211.
3. Chhabra A, Bajaj G, Wadhwa V, et al. MR Neurographic Evaluation of Facial and Neck Pain: Normal and Abnormal Craniospinal Nerves below the Skull Base. RadioGraphics 2018;38:1498–513.
4. Gfrerer L, Hansdorfer MA, Amador RO, et al. Muscle Fascia Changes in Patients with Occipital Neuralgia, Headache, or Migraine. Plast Reconstr Surg 2020;147:176–80.
5. Remy K, Hazewinkel MHJ, Knoedler L, et al. Etiologies of iatrogenic occipital nerve injury: And outcomes following treatment with nerve decompression surgery. J Plast, Reconstr Aesthetic Surg 2024;95:349–56.
6. Janis JE, Hatef DA, Ducic I, et al. The Anatomy of the Greater Occipital Nerve: Part II. Compression Point Topography. Plast Reconstr Surg 2010;126:1563–72.
7. Cruyssen FV der, Croonenborghs T-M, Renton T, et al. Magnetic resonance neurography of the head and neck: state of the art, anatomy, pathology and future perspectives. Br J Radiol 2021;94:20200798.
8. Kikuchi T, Fujii H, Fujita A, et al. Visualization of the greater and lesser occipital nerves on three-dimensional double-echo steady-state with water excitation sequence. Jpn J Radiol 2020;38:753–60.
9. Lin Y, Tan ET, Campbell G, et al. Improved 3D DESS MR neurography of the lumbosacral plexus with deep learning and geometric image combination reconstruction. Skelet Radiol 2024;53:1529–39.
10. Collick BD, Behzadnezhad B, Hurley SA, et al. Rapid development of application-specific flexible MRI receive coils. Phys Med Biol 2020;65:19NT01.
11. Abel F, Tan ET, Lunenburg M, et al. Flexible array coil for cervical and extraspinal (FACE) MRI at 3.0 Tesla. Phys Med Biol 2023;68:215011.
12. Rawner E, Trescot AM. Peripheral Nerve Entrapments, Clinical Diagnosis and Management. https://doi.org/10.1007/978-3-319-27482-9_19.
13. Hwang L, Dessouky R, Xi Y, et al. MR Neurography of Greater Occipital Nerve Neuropathy: Initial Experience in Patients with Migraine. Am J Neuroradiol 2017;38:2203–9.
14. Tubbs RS, Mortazavi MM, Loukas M, et al. Anatomical study of the third occipital nerve and its potential role in occipital headache/neck pain following midline dissections of the craniocervical junction: Laboratory investigation. J Neurosurg: Spine 2011;15:71–5.
15. Cesmebasi A, Muhleman MA, Hulsberg P, et al. Occipital neuralgia: Anatomic considerations. Clin Anat 2015;28:101–8.
16. Sneag DB, Queler SC, Campbell G, et al. Optimized 3D brachial plexus MR neurography using deep learning reconstruction. Skelet Radiol 2024;53:779–89.

SUPPLEMENTAL MATERIALS:

Online Supplemental Data: Summary of MR neurography findings and surgical outcomes in patients with occipital neuralgia using the FACE coil

No.	Age (years)	Sex	Surgical history	Laterality of occipital neuralgia (based on symptoms)	Approximate symptoms duration (months)	Acquired spatial resolution (mm)	MRN findings of GON	MRN findings of LON	MRN findings of TON	Other MRN findings	Treatment	Outcome
1	52	M	None	Right	7	0.6 × 0.6 × 0.8	No signal abnormality	No signal abnormality, but left side not visualized proximal to SCM	No signal abnormality	None	Nerve block targeting right C2-3 facet joint	No relief
2	36	F	None	Bilateral	48	0.6 × 0.6 × 0.6	No signal abnormality	No signal abnormality	No signal abnormality but bilateral not visualized proximal to	None	Bilateral GON decompression	Significantly improved

									semispinalis capitis			
3	52	M	None	Left	399	0.7× 0.7 × 0.8	No signal abnormality	no signal abnormality, but left side not visualized proximal to SCM	No signal abnormality	None	Left GON decompression	Resolved
4	35	M	Left occipital nerve decompression	Left	12	0.6 × 0.6 × 0.8	No signal abnormality	No signal abnormality	No signal abnormality	None	Left occipital trigger point injection	Partially improved
5	44	F	None	Bilateral	164	0.7 × 0.7 × 0.7	No signal abnormality	no signal abnormality, but bilateral side not visualized proximal to SCM	No signal abnormality	Trapezial fascia thickened	Bilateral occipital trigger point injection	No relief
6	70	M	Cervical spine surgery	Bilateral	26	0.7 × 0.7 × 0.7	Left GON terminal neuroma and right GON enlargement	No signal abnormality	No signal abnormality	None	Surgical neuroma excision	Significantly improved
7	73	F	Bilateral occipital nerve decompression	Bilateral	35	0.7 × 0.7 × 0.7	No signal abnormality	No signal abnormality	No signal abnormality	None	Conservative treatment	Partially improved
8	44	F	None	Left	10	0.7 × 0.7 × 0.7	No signal abnormality	No signal abnormality, but bilateral side not visualized proximal to SCM	No signal abnormality, but bilateral side not visualized proximal to semispinalis capitis	None	Nerve block targeting left GON, LON and TON	No relief
9	61	F	Cervical spine surgery	Bilateral	70	0.7 × 0.7 × 0.7	No signal abnormality	No signal abnormality, but bilateral side not visualized proximal to SCM due to cervical instrumentation.	No signal abnormality, but bilateral side not visualized proximal to C3 DRG due to cervical instrumentation.	None	Bilateral GON decompression	Resolved
10	69	M	Bilateral occipital nerve decompression	Bilateral	310	0.8 × 0.8 × 0.8	Right side neuroma	No signal abnormality	No signal abnormality	None	Nerve block targeting right GON, LON.	Partially improved
11	39	F	Left occipital nerve decompression	Left	131	0.7 × 0.7 × 0.7	Left side neuroma	No signal abnormality	Left side neuroma	None	Surgical neuroma excision and nerve transfer	Significantly improved
12	68	F	None	Right	336	0.8 × 0.8 × 0.8	No signal abnormality	Enlarged right LON	No signal abnormality	None	Nerve block targeting right GON, LON.	Significantly improved
13	67	F	Cervical spine surgery	Right	37	0.8 × 0.8 × 0.8	No signal	No signal abnormality	No signal abnormality	Hypertrophic remode	Referred for pain specialis	Lost follow up

		abnormality	ling of right C1-C2 right lateral mass articulation compressing right C2 DRG	t evaluation

*GON, greater occipital nerve; LON, lesser occipital nerve; TON, third occipital nerve; SCM, sternocleidomastoid muscle; DRG, dorsal root ganglion.